

Hydrodynamically Tunable Affinities for Fluidic Assembly

Mekala Krishnan,[†] Michael T. Tolley,[†] Hod Lipson,^{†,‡} and David Erickson^{*,†}

Sibley School of Mechanical and Aerospace Engineering and Computing and Information Science, Cornell University, Ithaca, New York 14853

Received October 22, 2008. Revised Manuscript Received December 3, 2008

Most current micro- and nanoscale self-assembly methods rely on static, preprogrammed assembly affinities between the assembling components such as capillarity, DNA base pair matching, and geometric interactions. While these techniques have proven successful at creating relatively simple and regular structures, it is difficult to adapt these methods to enable dynamic reconfiguration of the structure or on-the-fly error correction. Here we demonstrate a technique to hydrodynamically tune affinities between assembling components by direct thermal modulation of the local viscosity field surrounding them. This approach is shown here for two-dimensional silicon elements of 500 μm length using a thermorheological fluid that undergoes reversible sol–gel transition on heating. Using this system, we demonstrate the ability to dynamically change the assembly point in a fluidic self-assembly process and selectively attract and reject elements from a larger structure. Although this technique is demonstrated here for a small number of passive mobile components around a fixed structure, it has the potential to overcome some of the limitations of current static affinity based self-assembly.

1. Introduction

Self-assembly^{1,2} has been used to create structures at the micro- and nanoscales using techniques such as chemical bonding,^{3–5} fluid and surface tension based attraction,^{6–10} geometric interactions,^{11,12} and magnetic fields^{13,14} as the assembly driving mechanism. Most of these self-assembly processes create either highly regular structures such as colloidal crystals¹⁵ or small scale complex structures comprised of, for example, DNA polymers.¹⁶ Recently Chung et al.¹⁰ have developed a guided fluidic self-assembly process that allows for the assembly of relatively large irregular structures. Using this technique, the authors were able to design the assembling components on-the-fly and transport them on a railed network to the assembly site. While this technique is very flexible in the shape of the components, their motion is confined by the predefined rail networks on which these components move.

A hurdle to exploiting the potential of self-assembly is the inability of current techniques to assemble complex structures comprising large numbers of particles in nonregular, nonpredefined geometries. One of the reasons for this is the use of static interactions or affinities between the assembling components to drive the assembly process. For example, in nucleic-acid driven assembly, the final structure is governed by the predefined base-pair sequence.^{3,17} As a result, the assembling components and their affinities need to be specifically designed a priori for a given target structure. Since each affinity sequence corresponds to a specific target structure, assembled structures are also not generally reconfigurable. Similar arguments can be made for many hydrophobic/hydrophilic^{7,8,18} and geometric/surface tension interactions.^{11,12} In addition, static affinities also limit the complexity of the final target structure. This is because the number of patterns needed to uniquely specify any nonregular structure increases rapidly with structure size and consequently so does the complexity and number of the affinity patterns required to uniquely specify this structure. However, this increase in the number of required affinity patterns means that the difference between them or the specificity decreases. This leads to both slower assembly rates and increasing numbers of assembly errors. Error correction is similarly difficult to implement since the static affinities between components cannot be turned off to remove incorrectly assembled pieces.

One way to address the above issues is to develop a means to dynamically (i.e., during assembly) tune affinities between assembling components. The concept of affinity switching has been demonstrated at the centimeter scale using mechanical and magnetic switching.^{19–23} These methods however are difficult to implement at the microscale due to fabrication constraints and energy limitations. At the microscale, other researchers have attempted to switch the hydrophobicity of surfaces using electric potentials.²⁴ Gripping and releasing microstructures using electrowetting based techniques²⁵ has also been demonstrated. To date however these approaches have not been applied to

* To whom correspondence should be addressed.

[†] Sibley School of Mechanical and Aerospace Engineering.

[‡] Computing and Information Science.

(1) Philp, D.; Stoddart, J. F. *Angew. Chem.* **1996**, *35*(11), 1155–1196.

(2) Whitesides, G. M.; Grzybowski, B. *Science* **2002**, *295*(5664), 2418–2421.

(3) Winfree, E.; Liu, F. R.; Wenzler, L. A.; Seeman, N. C. *Nature* **1998**, *394*(6693), 539–544.

(4) Olenyuk, B.; Whiteford, J. A.; Fechtenkötter, A.; Stang, P. J. *Nature* **1999**, *398*(6730), 796–799.

(5) Rothmund, P. W. K. *Nature* **2006**, *440*(7082), 297–302.

(6) Bowden, N.; Terfort, A.; Carbeck, J.; Whitesides, G. M. *Science* **1997**, *276*(5310), 233–235.

(7) Bowden, N.; Arias, F.; Deng, T.; Whitesides, G. M. *Langmuir* **2001**, *17*(5), 1757–1765.

(8) Srinivasan, U.; Liepmann, D.; Howe, R. T. *J. Microelectromech. Syst.* **2001**, *10*(1), 17–24.

(9) Chung, J. H.; Zheng, W.; Hatch, T. J.; Jacobs, H. O. *J. Microelectromech. Syst.* **2006**, *15*(3), 457–464.

(10) Chung, S. E.; Park, W.; Shin, S.; Lee, S. A.; Kwon, S. *Nat. Mater.* **2008**, *7*(7), 581–587.

(11) Yeh, H. J.; Smith, J. S. *IEEE Photon. Technol. Lett.* **1994**, *6*(6), 706–708.

(12) Zheng, W.; Jacobs, H. O. *Appl. Phys. Lett.* **2004**, *85*(16), 3635–3637.

(13) Golosovsky, M.; Saado, Y.; Davidov, D. *Appl. Phys. Lett.* **1999**, *75*(26), 4168–4170.

(14) Tanase, M.; Silevitch, D. M.; Hultgren, A.; Bauer, L. A.; Searson, P. C.; Meyer, G. J.; Reich, D. H. *J. Appl. Phys.* **2002**, *91*(10), 8549–8551.

(15) Glotzer, S. C.; Solomon, M. J.; Kotov, N. A. *AIChE J.* **2004**, *50*(12), 2978–2985.

(16) Li, Y. G.; Tseng, Y. D.; Kwon, S. Y.; D'Espaux, L.; Bunch, J. S.; McEuen, P. L.; Luo, D. *Nat. Mater.* **2004**, *3*(1), 38–42.

(17) Yan, H.; Park, S. H.; Finkelstein, G.; Reif, J. H.; LaBean, T. H. *Science* **2003**, *301*(5641), 1882–1884.

(18) Chen, H. L.; Schulman, R.; Goel, A.; Winfree, E. *Nano Lett.* **2007**, *7*(9), 2913–2919.

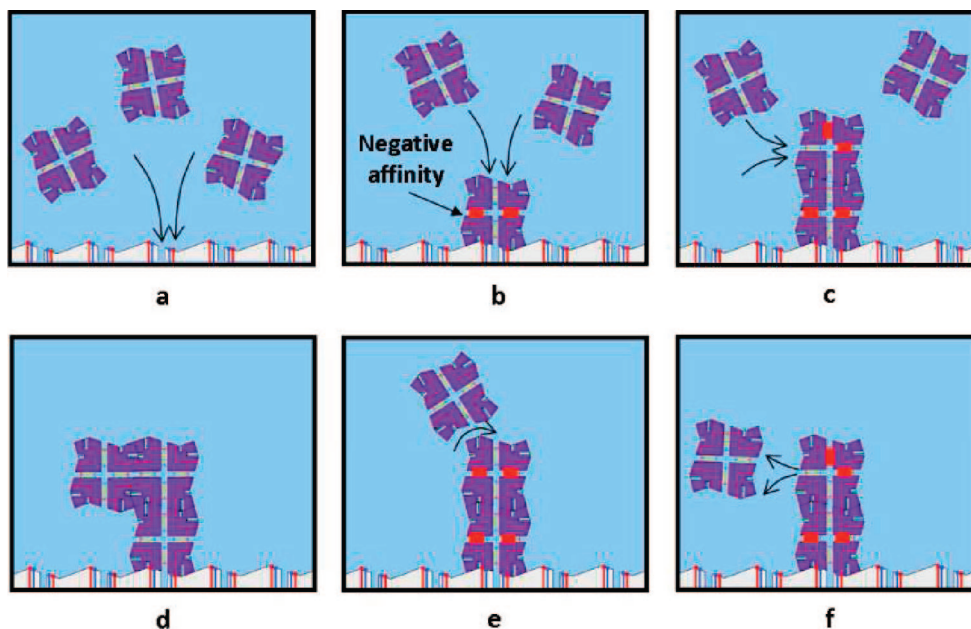


Figure 1. Schematic demonstrating the use of dynamically tunable affinities to create arbitrary, programmable, and reconfigurable structures. (a) The attraction of a subelement moving stochastically in the fluid to the substrate. The subelements are unpowered while in the fluid, but once they are attached to the substrate they can draw power to switch their affinities. (b, c) An arbitrary structure is built by dynamically switching the affinities within the structure and controlling the local attraction basin around the structure. (d) The final assembled structure. (e) Assembled structure is reconfigured by switching affinities. (f) Error correction: an incorrectly assembled component is rejected.

dynamically modulate affinities during self-assembly, and the binding strength of these bonds are typically low. Directed control over self-assembly has been demonstrated both thermorheologically²⁶ and electrochemically;²⁷ however, these methods have not been applied to affinity switching/tuning, assembly error correction, or structural reconfiguration. Dynamic self-assembly has been demonstrated through external manipulation of magnetic and electrostatic fields.²⁸ The resulting systems however are based on stable nonequilibrium configurations that remain ordered only as long as the systems continue to dissipate energy.

In this paper, we present a method to carry out the hydrodynamic tuning of attraction affinities between microscale assembly components using thermal modulation of the local flow field. We demonstrate the affinity tuning technique using a small set of mobile passive silicon components around a fixed structure and illustrate how it could be used to reconfigure structures, create different target structures from the same starting components and carry out error correction. As we describe in detail below, this is done using a thermorheological fluid that undergoes a reversible sol–gel transition on heating. This property of the fluid is used to modulate the local flow field around the mock component and thus tune intercomponent affinities. In addition to experimental results with the mobile silicon tiles, we also

characterized the affinity switching properties of the system using fluorescent polystyrene particles to visualize the local flow field and rhodamine B to study the thermal field.

Our process for affinity switching is shown in the schematic in Figure 1. In a fluidic self-assembly process, locally restricting the flow near one face of the structure limits the probability of another component being attracted to that face. Hence that part of the structure has no affinity for an approaching component, while other parts of the structure are still positive affinity regions. Figure 1 shows the use of affinity switching by flow modulation to create irregular structures, reconfigure structures, and carry out error correction.

While it is possible to use active flow control elements like valves on the assembling components to locally modulate flow, this requires significant component level fabrication. Instead, we employ “smart-fluids” which create self-assembled structures on the application of a suitable stimulus thus increasing the effective viscosity in the stimulated region. Our approach uses thermorheological fluids that undergo reversible sol–gel transition on heating. Other smart-fluids like electrorheological fluids²⁹ may also have been used, but we found that the particles were too big (on the order of 25 μm) and the required voltages too large (on the order of kilovolts per millimeter) for our purposes here.

To demonstrate the principle of hydrodynamically tunable affinities, we developed a structure consisting of a “mock” assembling component (or tile) with microchannels through it that is fixed in the microchamber where assembly is carried out. This represents a target structure that is being populated by further adding on approaching tiles to the existing structure. The mock tile was located in a microfluidic chamber³⁰ and a “mobile” silicon tile was introduced into the chamber for the experiments which we discuss below. The chamber was filled with a

(19) Murata, S.; Kurokawa, H.; Kokaji, S. *Proc. IEEE International Conference on Robotics and Automation (ICRA94)*, San Diego, CA, May 8–13, 1994.

(20) White, P.; Kopanski, K.; Lipson, H. *Proc. IEEE International Conference on Robotics and Automation (ICRA04)*, New Orleans, LA, April 26–May 1, 2004.

(21) Griffith, S.; Goldwater, D.; Jacobson, J. M. *Nature* **2005**, 437(7059), 636–636.

(22) Goldstein, S. C.; Cambell, J. D.; Mowry, T. C. *Computer* **2005**, 38(6), 99–101.

(23) Klavins, E. *IEEE Control Syst. Mag.* **2007**, 27(4), 43–56.

(24) Lahann, J.; Mitragotri, S.; Tran, T. N.; Kaido, H.; Sundaram, J.; Choi, I. S.; Hoffer, S.; Somorjai, G. A.; Langer, R. *Science* **2003**, 299(5605), 371–374.

(25) Vasudev, A.; Zhe, J. *Appl. Phys. Lett.* **2008**, 93(10), 103503:1103503:3.

(26) Sharma, R. *Langmuir* **2007**, 23(12), 6843–6849.

(27) Xiong, X. R.; Hanein, Y.; Fang, J. D.; Wang, Y. B.; Wang, W. H.; Schwartz, D. T.; Bohringer, K. F. *J. Microelectromech. Syst.* **2003**, 12(2), 117–127.

(28) Pelesko, J. *Self Assembly: The Science of Things That Put Themselves Together*, 1st ed.; Chapman & Hall/CRC: Boca Raton, FL, 2007; Chapter 7.

(29) Wen, W. J.; Huang, X. X.; Yang, S. H.; Lu, K. Q.; Sheng, P. *Nat. Mater.* **2003**, 2(11), 727–730.

(30) Tolley, M. T.; Krishnan, M.; Erickson, D.; Lipson, H. *Appl. Phys. Lett.* **2008**, 93(25), 254105:1 254105:3.

thermorheological fluid made of an aqueous solution of a triblock copolymer, poly(ethylene oxide)₁₀₆–poly(propylene oxide)₇₀–poly(ethylene oxide)₁₀₆ (see Materials and Methods section for details). Local heating of the thermorheological solution results in a rapid viscosity increase of the solution to reach a gel state, effectively shutting off flow in that region.^{31,32} On cooling, the gel returns to the liquid state and flow resumes. Affinity tuning by thermal flow modulation can take place by fabricating microheaters on board the assembling components. Here we focus on demonstrating the principle of hydrodynamic affinity tuning and thus pattern platinum microheaters under the channels of the fixed structure to modulate the local temperature field. In section 4, we discuss in detail the challenges involved in up scaling the technique to the case where mobile tiles would also contain local heaters. The heaters were designed by performing numerical analysis to ensure that they provided sufficient heating to cause gelation of the fluid (see Supporting Information for details on the simulations). Flow in the microchamber was driven using a pressure system and each of the microheaters was controlled independently using a voltage source and a relay arrangement.

2. Materials and Methods

2.1. Materials. We use a 15% (w/w) aqueous solution of Pluronic F127 (BASF) to make the thermorheological fluid. Pluronic F127 is triblock copolymer, poly(ethylene oxide)₁₀₆–poly(propylene oxide)₇₀–poly(ethylene oxide)₁₀₆, and a 15% solution has a gelation temperature of approximately 30 °C. The Pluronic F127 particles obtained from BASF were dissolved in DI water and left for 24 h in the refrigerator to dissolve the particles completely. The solution was brought to room temperature again prior to doing the experiments. We visualize the flow of the thermorheological fluid using suspended particles consisting of green fluorescent polystyrene particles of 0.72 μm diameter (Duke Scientific). Our microfluidic chamber was fabricated using polydimethylsiloxane (PDMS) obtained from Ellsworth Adhesives.

2.2. Fabrication. The microfluidic chamber used for our experiments was fabricated using standard photolithography techniques. A pyrex wafer was patterned with 30 nm of titanium and 150 nm of platinum to create the microheaters. This was followed by deposition of 250 nm of silicon nitride using plasma enhanced chemical vapor deposition to electrically insulate the thermorheological fluid from the heaters. The silicon nitride over the contact pads was then etched using reactive ion etching using photoresist as an etch mask for the other regions. The fluid layer was formed by first making a mold on a silicon wafer by deep silicon etching using a Bosch etching tool. PDMS was then poured over this mold and cured to fabricate a microfluidic chamber having a height of 50 μm. The PDMS layer was finally bonded to the pyrex substrate by plasma cleaning both layers, aligning, and leaving them overnight in a convection oven at 80 °C. The assembling tiles were made of 30 μm thick silicon from a silicon-on-insulator wafer using a deep Bosch etch followed by an HF release of the tiles.

2.3. Experimental Technique. The silicon tiles were stored in the thermorheological fluid and were pipetted into the microchamber. The thermorheological fluid was pumped into the microchamber through Tygon tubing using pressurized air at 0–5 psi. The pressure lines were controlled off-chip by solenoid valves and their controllers obtained from Fluidigm Corporation.

Each fluidic port in the chamber was subject to either a positive pressure (resulting in flow into the chamber) or no applied pressure (resulting in flow out of the chamber due to applied pressure at the other ports). The microheaters were controlled off-chip using a relay and data acquisition card obtained from Omega. Power was supplied to the heaters using a voltage supply of 0–30 V range obtained from Hewlett-Packard. Flow was visualized where needed using 0.72 μm fluorescent polystyrene beads obtained from Duke Scientific.

3. Results and Discussion

Figure 2a–d illustrates an experiment where the mobile tile was moved from one face of the mock tile to another by switching the affinity of the first face from positive to negative. The blue arrows in the figure illustrate the direction of flow during the reconfiguration process but not necessarily the relative magnitudes. The flow rates at each inlet port were equal since the applied pressure was fixed. The same applies at the outlet ports; however, in general, the inlet and outlet velocities were different in magnitude since the relative pressure difference was not the same. Local affinities on each face of the mock tile were disabled (or enabled) by turning the microheaters on (or off), increasing the probability of the mobile tile being attracted to one face over the others. The mobile tiles used in these experiments had a tendency to come toward their assembly point at a corner, and thus it was essential to use external flow manipulation (see the reversed flow used in Figure 2c) to ensure that the tiles aligned properly in their new position. In all cases, the tile was found to move toward the desired face, though the attraction affinity was not sufficient in all of the cases to cause the tile to completely switch positions to another face on the mock tile. The statistics of successful assembly events resulting from these manipulations are shown in Figure 2e for 10 consecutive trials of the same experiment. This experiment demonstrated the ability of tunable affinities to change the assembly point on the fly by manipulating the local flow field. This concept could in principle be used to carry out reconfiguration of a self-assembled structure. The video in the Supporting Information (1a803517f_si_002.mpg) shows a successful trial from this experiment.

We visualized the flow through the mock tile using fluorescent polystyrene beads and characterized the effect of the microheaters on the local flow velocity and gelation within the mock tile at different applied voltages. Figure 3a–c and the movie (1a803517f_si_003.mpg) in the Supporting Information show these results. This figure shows images from experiments where the pressure applied to the flow was 4 psi corresponding to a flow velocity through the channels in the tile of 1725 μm/s and different voltages were applied to the heater. Larger voltages resulted in larger regions of gelation around the heater as can be seen in these images. The variation of flow velocity through the heated channel and the characteristic length of gelation in the channel are shown in the graphs in parts d and e of Figure 3, respectively, for different driving pressures. From the graph in Figure 3d we see that voltages of 10 V and higher resulted in near zero flow velocity through the channel of the mock tile, thus achieving flow redirection and affinity switching. A voltage of 8 V was found to reduce the flow velocity from its original velocity but not stop flow completely, whereas voltages below 8 V resulted in no change in the flow (not shown in the graph). From Figure 3c and the graph in Figure 3e we see that at voltages above 12 V, the radius of the gelled region increased well beyond the channel dimension which is undesirable since gelation should occur only in the channel and not in the rest of the chamber. Figure 3f shows the time required to carry out complete redirection

(31) Wanka, G.; Hoffmann, H.; Ulbricht, W. *Macromolecules* **1994**, *27*(15), 4145–4159.

(32) Stoeber, B.; Yang, Z. H.; Liepmann, D.; Muller, S. J. *J. Microelectromech. Syst.* **2005**, *14*(2), 207–213.

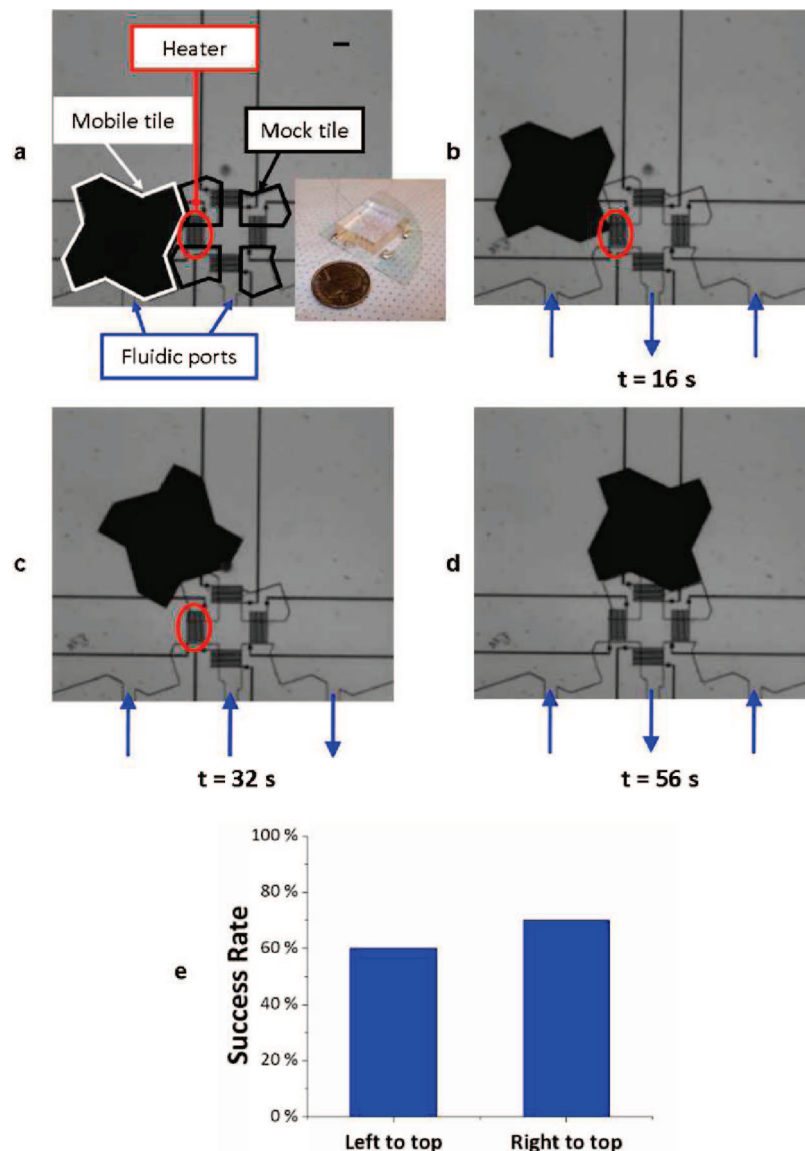


Figure 2. Change of assembly location by dynamically tuning affinities: (a) optical micrograph of the microfluidic assembly chamber. The chamber has a mock tile made of PDMS, a mobile tile made of silicon, platinum heaters, and fluidic ports. The inset image shows the final chip with electrical leads. The scalebar in the image is $100\ \mu\text{m}$. (b–d) Tile manipulation around the mock tile demonstrating the ability to reconfigure the final structure. A mobile silicon tile was moved around the mock tile by dynamically tuning the affinities at the faces of the mock tile through heater actuation. The blue arrows in the parts represent regions where flow enters or leaves the chamber, while the red circles show the heater being actuated. The blue arrows are representative of the direction of flow but not necessarily the magnitude. (e) Histogram showing percentage of successful tile assemblies for a mobile tile moving around the mock tile.

of flow and affinity switching at different voltages and driving pressures. As expected, the response time was found to decrease with increasing voltage. We also measured the temperature profile within the chamber at different voltages to ensure that the power provided by the heaters was sufficient to carry out gelation of the fluid and that the heat generation was localized. This was done in an aqueous medium, using rhodamine B dye for the thermal measurements.³³ The temperature measurements were carried out in a purely aqueous medium rather than in the polymer solution since the dye was found to change the gelation properties of the thermorheological fluid. Figure 3g shows the results from these experiments. A voltage of 10 V and above was found to locally heat the fluid to a temperature above $30\ ^\circ\text{C}$ and ensure that gelation takes place, though higher voltages were found to cause nonlocal heating. On the basis of these experiments, voltages between 10–12 V were used for our experiments for heater

actuation. We note here that the temperatures shown in Figure 3g are at steady state, implying that there is a balance between the energy input by the heaters and the heat loss through the chip. In this system, the majority of the heat loss is through the pyrex substrate, which has a higher conductivity compared to the upper PDMS fluidic layer.³³ Had we used a lower thermal conductivity substrate, the heat loss would have been lower and the required input energy would also be less. The higher thermal conductivity substrate however enables much more rapid dissipation of heat during the cooling phase and thus better switching times.

Having successfully demonstrated tile manipulation around the mock tile, we attempted to attract tiles from the far field flow (away from the mock tile structure) to a particular location on this tile depending on which of its faces was tuned to attract the mobile tiles, as can be seen from Figure 4. Although the external applied flow field was the same in these experiments, blockage of some of the channels of the mock tile resulted in increased

(33) Erickson, D.; Sinton, D.; Li, D. *Lab Chip* 2003, 3(3), 141–149.

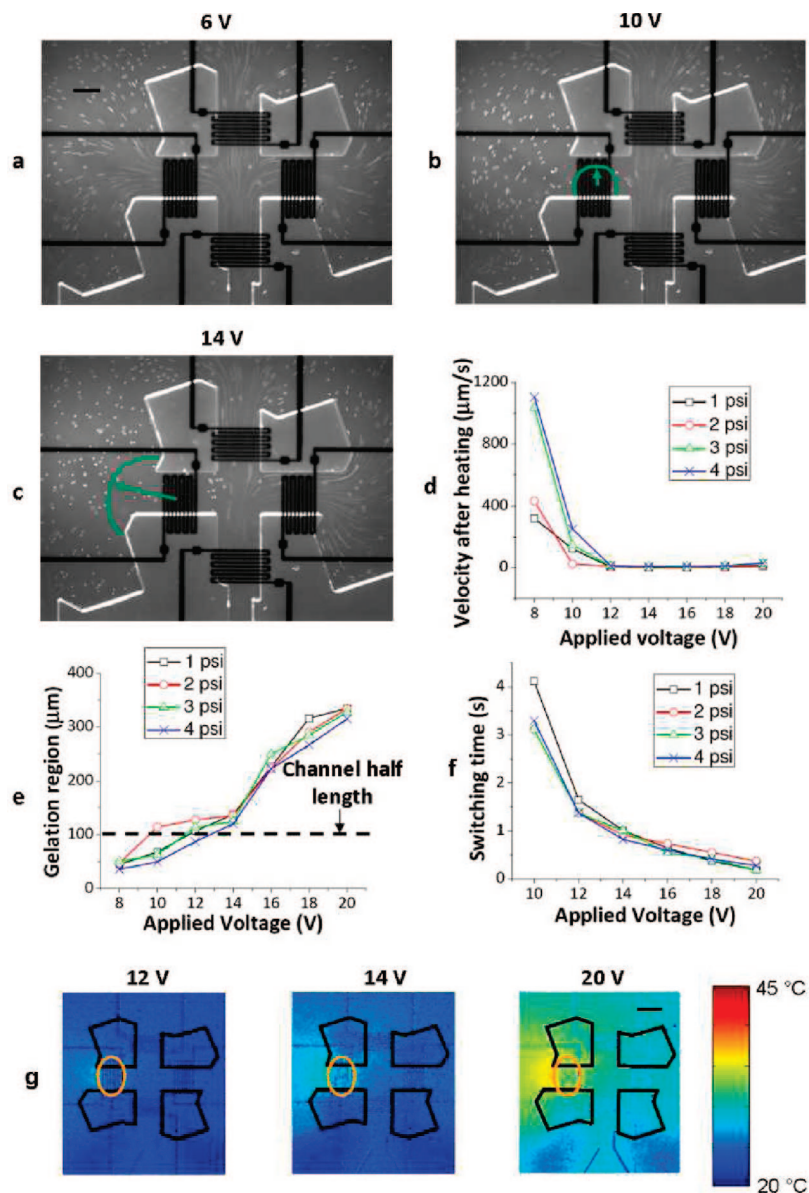


Figure 3. Characterization of hydrodynamic affinity tuning. (a–c) Images showing the effect of different voltages on the gelation region in the chamber. The scalebar in the image is 100 μm . The green curves show the region in the chamber that is gelled. (d) Graph showing the variation of flow velocity within the mock tile on heating at different heater voltages for different initial flow velocities. A voltage of 10 V and higher was found to stop flow within the channel of the mock tile. (e) Graph showing the characteristic length of the gelled region in the chamber for different heater voltages at different initial flow velocities. Voltages above 12 V were found to gel regions beyond just the channel which is undesirable. (f) Graph showing the response time of the thermorheological fluid for complete switching of flow, at different voltages and different initial flow rates. (g) Temperature profile in the microfluidic assembly chamber for different voltages, measured experimentally using rhodamine B. The legend indicates temperature in $^{\circ}\text{C}$, and the orange circles show the heaters being used. A voltage of 10 V and higher was found to raise the temperature sufficiently to cause gelation and affinity switching.

flow rate through the open channels of the tile. We note that the mock structure is not affected by the changes in the flow as it is permanently affixed to the substrate (analogous to being latched on as is demonstrated in Tolley et al.³⁰). The mobile tile was attracted to different faces on the mock structure depending on which of the microheaters was actuated, even though the same external flow field was applied in all these experiments. We did find that the mobile tile did not align well to the mock structure in all cases since, as mentioned previously, this tile shape was found to inherently come toward its assembly point on a corner. Such a technique could be applied to a fluidic assembly process to create different target structures from identical initial components and thus allow for programmable assembly. The video (la803517f_si_004.mpg) in the Supporting Information contains all the above experimental results.

As a final experiment, we attempted to assemble nonregular structures with two mobile tiles, and a two tile mock structure as shown in Figure 5. Figure 5a shows the assembly of such a structure by tuning the affinities of the mock tiles. One mobile tile is first brought in to form a three tile shape (not shown here) followed by the attraction of a second mobile tile to form a nonregular assembly consisting of four tiles. Other four tile polymorphs were also assembled such as the initial structure in Figure 5c. We also studied switching intertile affinities to reject assembled tiles from the main structure as shown in Figure 5b,c. In these figures we show results from experiments where a mobile tile was rejected from the assembly, keeping the other tile in place, resulting in a new three tile assembly. Although demonstrated here using a fixed mock tile and passive mobile tiles, such an approach could be adapted to carry out error correction

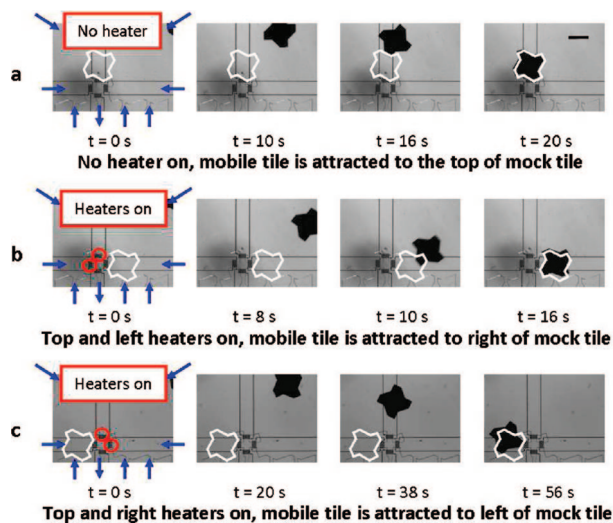


Figure 4. Images showing the formation of different final structures by dynamically tuning affinities of the mock tile. The blue arrows show regions where flow enters or leaves the chamber, the red circles show the heaters being actuated, and the white tiles show the target position in each case. (a) With no heater action, the mobile tile was attracted to the top of the mock tile forming a vertical column structure. The scalebar in the image is $500 \mu\text{m}$. (b) With the top and left heaters on, the mobile tile was attracted to the right of the mock tile forming a horizontal row structure. (c) With the top and right heaters on, the mobile tile was attracted to the left of the mock tile forming a horizontal row structure different from that formed in part b.

in a fluidic assembly process by selectively removing incorrectly assembled units from the main structure. Videos of the above experiments are provided in the Supporting Information video (la803517f_si_005.mpg).

4. Summary and Conclusions

In conclusion, we have demonstrated here the ability to hydrodynamically tune affinities between assembling components using a thermorheological fluid. Unlike self-assembly methods based on static affinities, the technique of tunable affinities presented here has the potential to one day allow the assembly of arbitrary, nonpredefined, and reconfigurable target structures. Such an assembly method could allow for interesting applications such as self-healing structures, tunable electronics, and displays.

A challenge to scaling our assembly method to a large number of elements is slow assembly rates due to the need to tune affinities at each stage of the assembly process. This could be overcome by carrying out parallel, hierarchical assembly as well as combining static affinity based assembly approaches (for carrying out coarse assembly) with dynamic affinity tuning (for fine assembly to describe detailed features on the target structure). Although we have demonstrated the ability to fabricate tiles with electrical and mechanical functionality,³⁴ another possible limitation is the complex control schemes needed to operate the heaters for affinity switching during assembly. However, even

(34) Tolley, M. T.; Baisch, A.; Krishnan, M.; Erickson, D.; Lipson, H. *Proceedings of the 21st IEEE International Conference on Micro Electro Mechanical Systems (MEMS)*, Tucson, AZ, Jan 13–17, 2008.

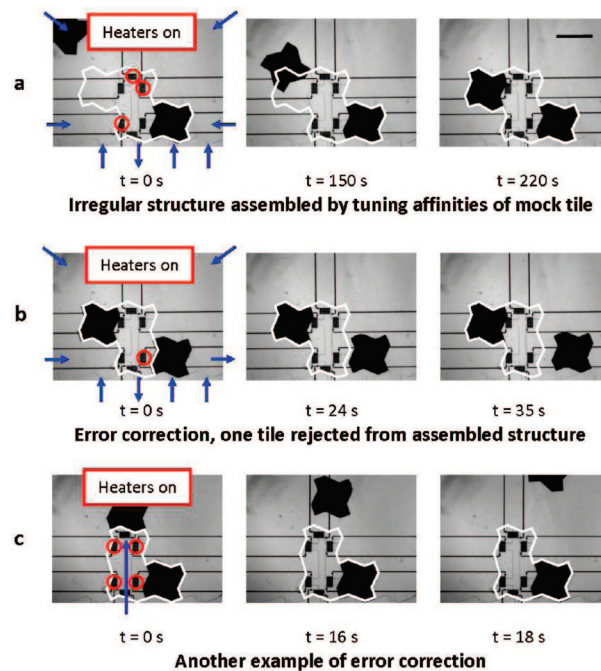


Figure 5. Images showing the formation of irregular structures and techniques for error correction. The blue arrows show regions where flow enters or leaves the chamber, the red circles show the heaters being actuated, and the white lines show the target structure in each case. (a) An irregular structure consisting of two mobile tiles and a two tile mock structure was formed by selectively tuning affinities. The scalebar in the image is $500 \mu\text{m}$. (b) One mobile tile was rejected selectively from this assembled structure (while keeping the other tile in place) demonstrating a means to carry out error correction. (c) Another example of error correction showing the rejection of one tile from the assembled structure while keeping the other tile in place.

though the number of heater control lines scales linearly with the number of elements (with four control lines per two-dimensional element), the affinities of only the outer layer of the structure need to be controlled at each level of assembly as new layers are added to the structure. Hence the control scheme for this assembly process does not need to involve all the elements of the assembled structure and can thus be relatively simple. Additionally, combining static and dynamic assembly approaches as mentioned above will further simplify the control schemes required to carry out assembly.

Acknowledgment. This work was supported by the Defense Advanced Research Projects Agency (DARPA), Defense Sciences Office (DSO) under the Programmable Matter program, and the National Science Foundation (NSF) under Grant No. CMMI-0634652, "Hierarchical Microfabrication: Actively Programmable Multi-level Fluidic Self-Assembly."

Supporting Information Available: Details of numerical simulations performed to design the heaters used in the experiments and supplementary movies showing the experiments that have been described above. This material is available free of charge via the Internet at <http://pubs.acs.org>.

LA803517F